SATELLITE DOCKING SIMULATOR BASED ON HARDWARE-IN-THE-LOOP HYBRID CONTACT MODEL

M. Zebenay[1], T. Boge[1], R. Lampariello[2], and D. Choukroun[3]

[1]*Institute of German Space Operations Center, DLR, 82234 Weling, Germany*
[2]*Institute of Robotics and Mechatronics, DLR, 82234 Weling, Germany*
[3]*Department of Space Engineering, Delft University of Technology , 2629 HS Delft The Netherlands*

ABSTRACT

This paper briefly presents a hardware-in-the-loop (HIL) docking simulator concept. A critical requirement for the docking simulation of the HIL simulator is that its 6-degree of freedom (DOF) robots have to mimic the dynamic response of two satellites during contact/docking. However, the closed-loop response is influenced by the time delay of the robots controller, as well as by the robots high structural stiffness. This effects gives rise to unrealistically high impact forces, which not only jeopardize the safety of the facility, but also introduce a non-deterministic error in the docking simulation. Furthermore, the controller time delay will generally destabilize the HIL simulation. In order to mitigate these undesired effects, a new tool for emulating impacts is presented, which is based on a combination of passive and active compliance. This approach ensures safe operation of the simulation facility and also allows to reproduce impact dynamics with different values of stiffness and damping characteristics. This paper presents the extension of the method for more than one dimension. In addition, this paper presents the effect of parameters which are time delay, stiffness, damping and masses of the simulating satellites on the stability of the HIL docking simulator. The method is validated in simulation.

Key words: Hybrid contact dynamics model; High-stiffness; Time-delay.

1. INTRODUCTION

Ground proximity operation simulators have been used for satellite control verification since the beginning of space programme [1]. Even if, there exist many technologies available for testing and verification in a simulated micro-gravity environment such as free-fall methods, air-bearing tables, neutral Buoyancy, suspended systems, underwater test tanks and HIL simulator, only the HIL simulator have proven useful for RvD testing in 6-degrees of freedom. On the other hand, robotics-based hardware-in-the-loop simulators implement effective active gravity compensation, can accommodate complex systems for the RvD simulation, and enable full translation and rotational motions. There are several examples of HIL simulators for space systems RvD simulation [3][5][6].

The DLR has upgraded the old version of European Proximity Operation Simulator (EPOS) facility which was used for GNC test and verification by an entirely new facility as the design concept shown in Fig. 1 [4]. The unique features of this new facility, in comparison with the previously described simulators, are the two heavy-duty industrial robots. These robots can handle payloads up to 250 kg. In addition, the facility allows relative motion between the robots with a range up to 25m. The new EPOS facility is aimed at providing test and verification capabilities for complete RvD procedures of on-orbit servicing missions [3].

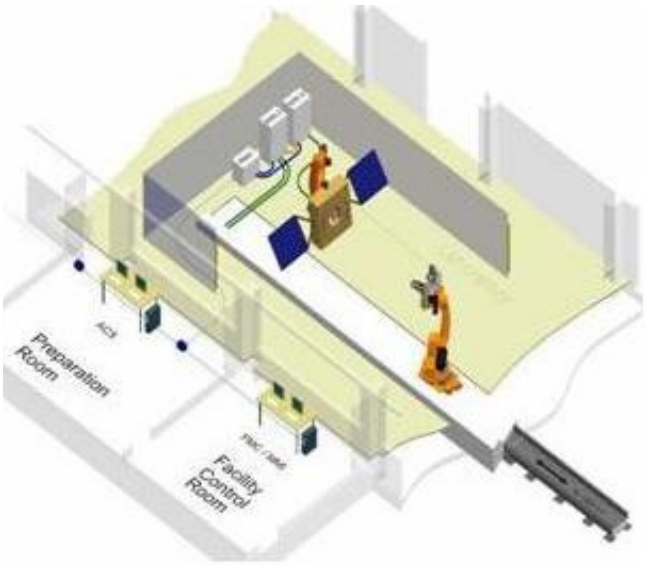

Figure 1. The EPOS facility: two robots (in orange), one holding a satellite mock-up (left), the other mounted on a rail (right); control room and preparation room

Figure 2 shows the main components of the HIL docking simulator concept. The concept schematic consists of three basic subsystems:

- a real-time numerical satellite dynamics simulator: the input to the simulator are the robots measured positions and the measured force and torque during contact.
- two industrial 6-DOF robots: the robots are commanded in position using the inputs from the simulator. They react with a 16ms delay and settle their end-effectors on the desired positions.
- a hardware mock-up of the docking mechanisms on the satellites, which will make physical contact operations during docking and capturing.

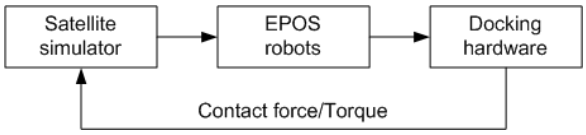

Figure 2. Main components of an HIL docking simulator concept

Using industrial robots for the HIL docking simulator is a highly challenging approach because these robots are designed as accurate positioning machines. As such, they are typically very stiff and do not naturally comply with the particular contact dynamics that satellite boundaries experience during contact. In addition, initially designed for typical industrial applications their speed of response is slow for high stiffness contact task.

In order to mitigate the problems, *hybrid contact dynamics emulation method* was presented [2]. The method was validated both in simulation and in experiment using EPOS facility. The result validated the docking simulator concept using EPOS facility. However, the method requires to design a passive compliance device that shall be mounted between the docking interface and robot end-effector. In addition, the method shall be extended to more than 1D.

In this paper, the extension of 1D *hybrid contact dynamics emulation method*[2] is presented that alleviates the need to change the passive compliance. It consists of combining a real passive compliance between the robot end-effector and the docking interface with a virtual contact dynamics model in the satellite numerical simulator. The advantage of this method is that the real passive compliance can remain unchanged while the virtual contact model can be tuned to arrive at the desired stiffness characteristics. The effect of the passive compliance is to lengthen the duration of the impact, thus avoiding the undesired consequences of the aforementioned time delay, but at the loss of some accuracy in position. The paper also presents the passive compliance device design and its kinematics analysis.

We begin with the dynamics model of the satellites in contact. Then, the development of the *hybrid contact dynamics emulation method* is presented. It is followed by a through stability analysis of the method. Finally, the simulation result is presented before the conclusion.

2. DYNAMICS MODEL OF RIGID SATELLITES IN CONTACT

The dynamics models of the two docking satellites can be conveniently expressed in the body frames for the Chaser satellite *D* and Target satellite *T* defined at its center of masses (CoM). Fig. 3 shows the frames and the concept of HIL docking simulator. The satellites can be assumed purely as a free-floating object, i.e., the effect of earth gravity is neglected. When the two satellites are in proximity distance for docking along the V-bar direction, they are in the same orbit. Thus, the celestial mechanics effect is negligible in comparison with the contact forces during docking operation. Therefore, the orbital frame can be assumed to be an inertial frame *G* because the orbital dynamics has been ignored [8].

Consider the satellites translational and rotational motions are described in the body fixed frames *D* and *T* which are chosen at the center of masses of the satellites **CoM**. Assume all quantities are expressed in the coordinate frame *D* for the Chaser dynamics model and *T* for the Target dynamics model , unless otherwise is specified. $\mathbf{f}_c^{D,T}$ and $\boldsymbol{\tau}_c^{D,T}$ denote the component of the contact force $\mathbf{f}_c$ and contact torque $\boldsymbol{\tau}_c$ defined at the frames *D* for the Chaser and *T* for the Target respectively. Moreover, $\mathbf{v}_c^{D,T}$ is the components of the linear velocity of the **CoM** of the Chaser or Target and $\boldsymbol{\omega}_c^{D,T}$ is the angular velocity expressed in *D* or *T*. Assume that $m_{D,T}$ and $\mathbf{I}^{D,T}$ denote the satellite masses and inertia tensors expressed in frames *D* and *T*.

Using Newton-Euler equations the dynamics of the Chaser satellite simulator are given with respect the frame *D* as [9]:

$$\begin{bmatrix} m_D E & 0 \\ 0 & \mathbf{I}^D \end{bmatrix} \begin{bmatrix} \dot{\mathbf{v}}_c^D \\ \dot{\boldsymbol{\omega}}_c^D \end{bmatrix} + \begin{bmatrix} \boldsymbol{\omega}_c^D \times m_D \mathbf{v}_c^D \\ \boldsymbol{\omega}_c^D \times \mathbf{I}^D \boldsymbol{\omega}_c^D \end{bmatrix} = \begin{bmatrix} \mathbf{f}_c^D \\ \boldsymbol{\tau}_c^D \end{bmatrix} \quad (1)$$

where E is the 3×3 identify matrix and the derivate is relative to the body frame.

Similarly for the Target satellite dynamics model can be written as:

$$\begin{bmatrix} m_T E & 0 \\ 0 & \mathbf{I}^T \end{bmatrix} \begin{bmatrix} \dot{\mathbf{v}}_c^T \\ \dot{\boldsymbol{\omega}}_c^T \end{bmatrix} + \begin{bmatrix} \boldsymbol{\omega}_c^T \times m_T \mathbf{v}_c^T \\ \boldsymbol{\omega}_c^T \times \mathbf{I}^T \boldsymbol{\omega}_c^T \end{bmatrix} = \begin{bmatrix} \mathbf{f}_c^T \\ \boldsymbol{\tau}_c^T \end{bmatrix} \quad (2)$$

2.1. Contact dynamics model

In the derivation of the dynamics of two satellites in contact, contact modeling is an important issue. The general form of the continuous contact normal force, f_n, modeling can be formulated as follows [11] [12]:

$$f_n = k_c \delta x^n + b_c g(\delta x) \delta \dot{x}^q \quad (3)$$

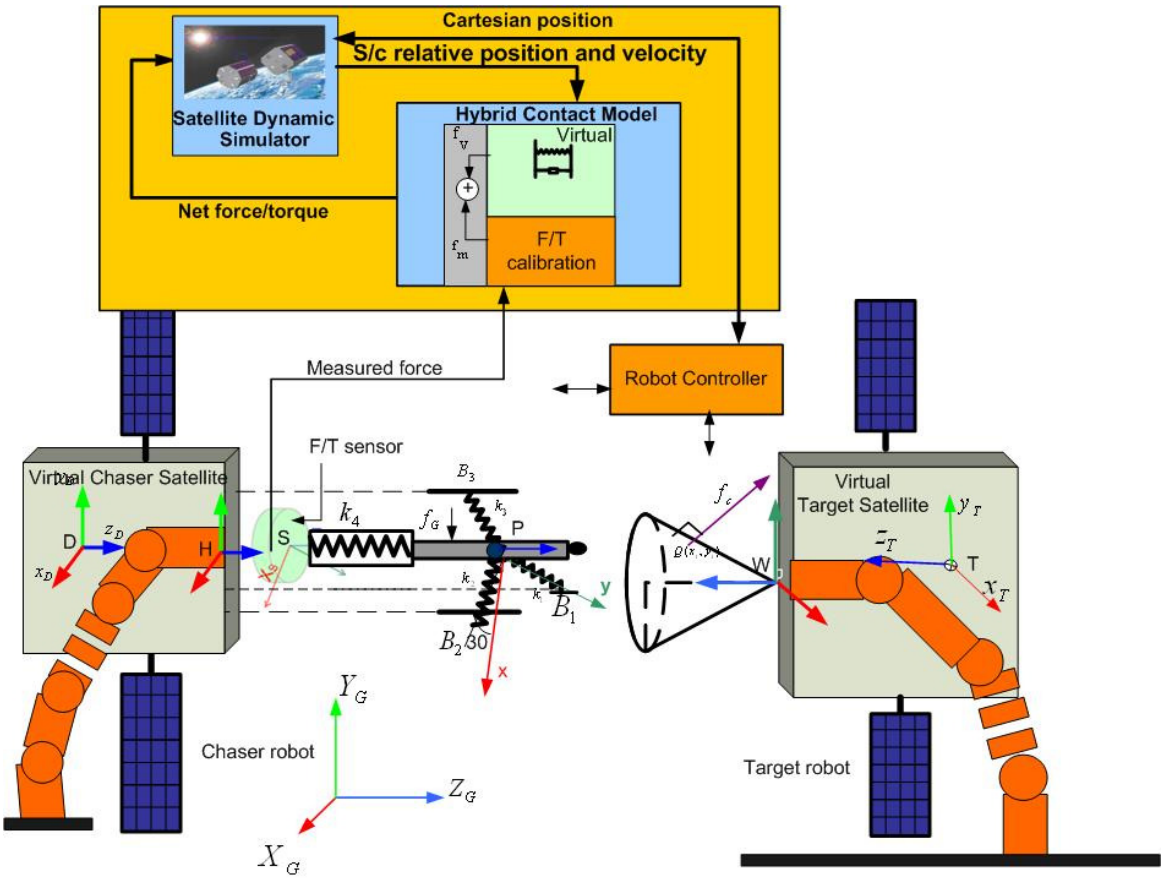

Figure 3. Schematics of the hardware-in-the-loop docking simulator consists of: two position controlled robots, Passive compliance device, F/T sensor and docking interfaces

where δx is the relative position or penetration between the contacting bodies, b_c is the damping coefficient of the contacting surfaces, k_c is the stiffness of the contacting surfaces. From (3), when $g(\delta x) = q = n = 1$ the contact model is called spring-dashpot model. This model is a popular choice due to its simplicity [10] [11] [12]. This work also adopts the spring-dashpot model. Thus the contact force f_n is modeled as:

$$f_n = k_c \delta x + b_c \delta \dot{x} \tag{4}$$

3. HYBRID CONTACT DYNAMICS MODEL

In this section, we present an extension of the novel hybrid contact dynamics model from 1-DOF [2] to 6-DOF that alleviates the need to change the passive compliance for each docking scenarios. It consists of combining a real passive compliance between the robot end-effector and the docking interface with a virtual contact dynamics model in the satellite numerical simulator. The advantage of this method is that the real passive compliance can remain unchanged while the virtual contact model can be adapted to arrive at the desired stiffness or damping characteristics.

Section 3.1 presents the dynamics of the designed passive compliance device and section 3.2 presents how the hybrid contact model computes the net contact force.

3.1. Dynamics of the new passive compliance device

Fig 4 shows the schematics diagram of the docking interface device. The top view shows the three equal legs connected at a point. The angles made by the three legs at the connection point are equal. The fourth leg is perpendicular to the three legs and passes through the connection point. During contact the legs deforms proportionally to the magnitude of the contact force. The measurement of the deformation of the legs enables us to determine the external forces through force transformation matrix. Even if we use force/torque sensor to measure the contact force, the transformation matrix is derived below for the purpose of developing the hybrid contact model concept.

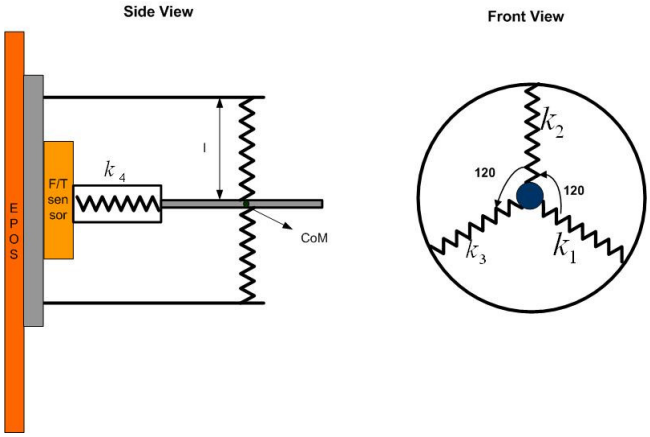

Figure 4. Kinematic Structure of the docking interface

From Fig. 3, consider $\mathbf{x} = (x, y, z)$ which is the location of point P with respect to frame *S*, $B_i = (X_{Bi}, Y_{Bi}, Z_{Bi})$ as the location of points B_i with respect to frame *S* and l_i is the initial length of the springs where $i = 1, 2, 3, 4$.

Define leg i as a vector of $\mathbf{l}_i$:

$$\mathbf{l}_i^S = \begin{bmatrix} l_{iX} \\ l_{iY} \\ l_{iZ} \end{bmatrix} = P - B_i = \begin{bmatrix} x - X_{Bi} \\ y - Y_{Bi} \\ z - Z_{Bi} \end{bmatrix} \tag{5}$$

The length of leg i, is given by:

$$\mathbf{l}_i^S = \mid \mathbf{x} - B_i \mid = \sqrt{l_{iX}^2 + l_{iY}^2 + l_{iZ}^2} \tag{6}$$

And define a leg vector as $\mathbf{l}^S = [\mathbf{l}_1\ \mathbf{l}_2\ \mathbf{l}_3\ \mathbf{l}_4]^T$. Furthermore, define a Jacobian matrix $\mathbf{J}$ that relates a point P deflection, $\delta\mathbf{x}$ and leg deflection $\delta\mathbf{l}$ by:

$$\delta\mathbf{l} = \mathbf{J}\delta\mathbf{x} \tag{7}$$

where $\delta\mathbf{x} = (\delta x, \delta y, \delta z)$.
Thus $\mathbf{J}$ is:

$$\mathbf{J} = \frac{\partial \mathbf{l}}{\partial \mathbf{x}} = \begin{bmatrix} \frac{\partial l_1}{\partial x} & \frac{\partial l_1}{\partial y} & \frac{\partial l_1}{\partial z} \\ \frac{\partial l_2}{\partial x} & \frac{\partial l_2}{\partial y} & \frac{\partial l_2}{\partial z} \\ \frac{\partial l_3}{\partial x} & \frac{\partial l_3}{\partial y} & \frac{\partial l_3}{\partial z} \\ \frac{\partial l_4}{\partial x} & \frac{\partial l_4}{\partial y} & \frac{\partial l_4}{\partial z} \end{bmatrix} \tag{8}$$

where

$$\frac{\partial l_i}{\partial x} = \frac{x - X_{B_i}}{l_i} = \frac{\delta x_i}{l_i} \tag{9}$$

$$\frac{\partial l_i}{\partial y} = \frac{y - Y_{B_i}}{l_i} = \frac{\delta y_i}{l_i} \tag{10}$$

$$\frac{\partial l_i}{\partial z} = \frac{z - Z_{B_i}}{l_i} = \frac{\delta z_i}{l_i} \tag{11}$$

Neglecting gravity and friction, the force felt at each leg is computed from the leg deflection and the stiffness of each leg.

$$F_{l_i} = k_i \delta l_i \tag{12}$$

The force vector at each leg can be written in vector form as:

$$\mathbf{f_l} = \mathbf{K}\delta\mathbf{l} = \mathbf{K}\mathbf{J}\delta\mathbf{x} \tag{13}$$

where $\mathbf{K}$ is 4×4 diagonal matrix given by:

$$\mathbf{K} = \begin{bmatrix} k_1 & 0 & 0 & 0 \\ 0 & k_2 & 0 & 0 \\ 0 & 0 & k_3 & 0 \\ 0 & 0 & 0 & k_4 \end{bmatrix} \tag{14}$$

Simplifying the equation above, we model the force for each leg as:

$$\mathbf{f}_{l_i}^S = k_i(\frac{\delta x_i}{l_i})\delta x + (\frac{\delta y_i}{l_i})\delta y + (\frac{\delta z_i}{l_i})\delta z) \tag{15}$$

Thus the model of the contact force measured by the force/torque sensor is the sum of forces due to each spring deflection which is computed as:

$$\mathbf{f}^S = \sum \mathbf{f}_{l_i}^S \tag{16}$$

3.2. Net Contact force

The hybrid contact model force is computed by adding the force/torque sensor measurement and virtual contact model force. The determination of the virtual contact model parameters is based on the assumed knowledge of the stiffness matrix, $\mathbf{K}$ and the infinitesimal damping value of the compliance device. Rewriting Eq. 16 in there corresponding axis:

$$\mathbf{f}^S = \begin{bmatrix} f_x \\ f_y \\ f_z \end{bmatrix} \tag{17}$$

$$\begin{bmatrix} f_x \\ f_y \\ f_z \end{bmatrix} = \begin{bmatrix} k_1(\frac{\delta x_1}{l_1})\delta x + k_2(\frac{\delta x_2}{l_2})\delta x + k_3(\frac{\delta x_3}{l_3})\delta x \\ k_1(\frac{\delta y_1}{l_1})\delta y + k_2(\frac{\delta y_2}{l_2})\delta y + k_3(\frac{\delta y_3}{l_3})\delta y \\ k_1(\frac{\delta z_1}{l_1})\delta z + k_2(\frac{\delta z_2}{l_2})\delta z + k_3(\frac{\delta z_3}{l_3})\delta z + k_4\delta z \end{bmatrix} \tag{18}$$

Here we propose to add the virtual contact model parallel to each axis. Fig 5 shows the concept of the hybrid contact model along the probe axis. Thus the net contact force $\mathbf{f}_c$ with respect to frame *S* is:

$$\mathbf{f}_c^S = \mathbf{f}_v^S + \mathbf{f}^S \tag{19}$$

Using spring-dashpot contact force modeling of Eq. 4, the virtual contact force is computed along each axis as:

$$\mathbf{f}_v^S = \begin{bmatrix} f_{vx} \\ f_{vy} \\ f_{vz} \end{bmatrix} = \begin{bmatrix} k_{vx}\delta x + b_{vx}\delta \dot{x} \\ k_{vy}\delta y + b_{vy}\delta \dot{y} \\ k_{vz}\delta z + b_{vz}\delta \dot{z} \end{bmatrix} \tag{20}$$

Eq. (19) allows the user to tune the virtual stiffness and

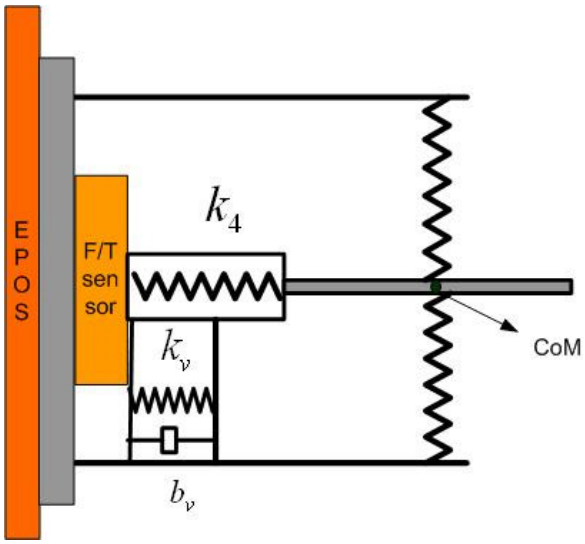

Figure 5. Schematics of the hybrid contact model on the probe axis: Passive stiffness k_4 and the virtual stiffness k_v and virtual damping b_v

the damping to match the desired contact parameters or force profile. Note however that the desired stiffness is limited by the sampling time of the robotic facility: only impacts with a time duration which is some multiples of this sampling time can be simulated correctly. The new passive compliance device is designed by assuming the desired contact parameters for contact simulation are always higher than the device contact parameters. Thus, the virtual impedance should be virtually connected to the device in parallel where the values can be computed analogies to a Series connected electrical network resistors. For example, assume the desired net contact parameters at the legs are equal to stiffness of k_{cx}, k_{cy}, k_{cz} and damping of b_{cx}, b_{cy}, b_{cz}. Thus the virtual component is computed as:

$$\begin{bmatrix} k_{vx} \\ k_{vy} \\ k_{vz} \end{bmatrix} = \begin{bmatrix} k_{cx} - k_x \\ k_{cy} - k_y \\ k_{cz} - k_z \end{bmatrix} \tag{21}$$

$$\begin{bmatrix} b_{vx} \\ b_{vy} \\ b_{vz} \end{bmatrix} = \begin{bmatrix} b_{cx} \\ b_{cy} \\ b_{cz} \end{bmatrix} \tag{22}$$

where

$$k_x = k_1(\frac{\delta x_1}{l_1}) + k_2(\frac{\delta x_2}{l_2}) + k_3(\frac{\delta x_3}{l_3}) \tag{23}$$

$$k_y = k_1(\frac{\delta y_1}{l_1}) + k_2(\frac{\delta y_2}{l_2}) + k_3(\frac{\delta y_3}{l_3}) \tag{24}$$

$$k_z = k_1(\frac{\delta z_1}{l_1}) + k_2(\frac{\delta z_2}{l_2}) + k_3(\frac{\delta z_3}{l_3}) + k_4 \tag{25}$$

In order simulate the HIL docking simulator, it is required to feedback the contact forces with the appropriate frames of the Chaser satellite and the Target satellite. The net contact force of the hybrid contact model can be transformed to the frame D as:

$$\mathbf{f}_c^D = \mathbf{R}_D^S \mathbf{f}_c^S \tag{26}$$

where $\mathbf{R}_D^S$ is the rotation matrix from frame *S* to frame *D* and the contact torque with respect to frame D is:

$$\boldsymbol{\tau}_c^D = \mathbf{r}_{DQ} \times \mathbf{f}_c^D \tag{27}$$

where $\mathbf{r}_{DQ}$ is a vector from the center of mass of the Chaser satellite to the contact point Q.

Similarly the contact force can be transformed to the Target frame T as:

$$\mathbf{f}_c^T = \mathbf{R}_T^S \mathbf{f}_c^S \tag{28}$$

where $\mathbf{R}_T^S$ is the rotation matrix from frame *S* to frame *T* and the contact torque with respect to frame T is:

$$\boldsymbol{\tau}_c^T = \mathbf{r}_{TQ} \times \mathbf{f}_c^T \tag{29}$$

where $\mathbf{r}_{TQ}$ is a vector from the center of mass of the Target satellite to the contact point Q.

4. STABILITY ANALYSIS OF THE HIL DOCKING SIMULATION CONCEPT

The previous section presents the hybrid contact model where the user is allowed to tune the virtual stiffness and damping. As a result of the tuning, it is possible to change the force profile and contact frequency. However, the range of allowed contact frequency is limited due to the bandwidth limit and time delay of the robot controller. Thus, it is required to identify a stable region of the simulator as a function of contact stiffness, damping, time delay and mass of the satellites. This section presents an analytical solution for 1D case.

For the case of 1D contact case the two satellites are modeled by two masses connected by a spring and a damper, where the contact force is modeled using a linear spring-dashpot method. The magnitude of the contact force is computed as follows:

$$f_c = k_c\delta x + b_c\delta \dot{x} \tag{30}$$

where δx stands for the relative position between the two masses during contact, k_c is a contact body stiffness and

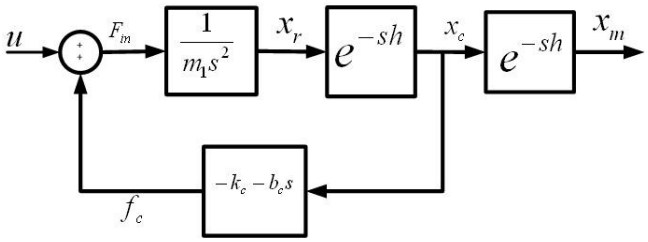

Figure 6. Simplified transfer function block diagram of the simulator

b_c is a velocity proportional damper.
When the HIL docking simulation concept is implemented such as in the EPOS facility, it has a closed-loop system as shown in Fig. 6 where the robots are modeled by a time delay of the controller. The transfer function of the HIL docking simulator is modeled as Eq. 31 where h is the time delay of the robots controller before the robots respond to the command.

$$H(s) = \frac{X_m(s)}{U(s)} = \frac{\frac{1}{m_1 s^2} e^{-s2h}}{1 + e^{-sh}\frac{k_c + b_c s}{m_1 s^2}} \tag{31}$$

$$m_1 = \frac{m_S m_T}{m_S + m_T} \tag{32}$$

where $X_r(s)$ is the required position command from the free-floating model, $X_c(s)$ is the current position of the robot end-effector, $X_m(s)$ is the measured position of the end-effector and $F_c(s)$ is the net contact force.

The stability analysis for Eq 31 was performed using Routh's Criterion by approximating the time delay [2]. In this section stability window is computed analytically without approximation of time delay function into rational function.

One way to answer the stability question with time delay in the loop, h, is studying the behavior of the system roots as h increases from zero to the delay value [13]. The condition for stability is that all the roots of the characteristic equation:

$$C(s,h) = D(s) + N(s)e^{-sh} = 0 \tag{33}$$

lie in the left half of the complex s-plane. The basic problem of stability is to determine the ranges of values of h for which the system is stable. Walton and Marshall [13] have presented three steps procedure to study the stability of the system with time delay. By adapting these procedures, we identify the stability window of Eq. 31 as a function of k_c, b_c, m_1 and h.

Thus the system is stable if the time delay is in the following range for a given value of stiffness, k_c, damping, b_c, reduced mass, m_1.

$$0 < h < h_0 \tag{34}$$

where the crossover frequency, ω_c is:

$$\omega_c^2 = \frac{b^2}{4m_1^2} + \frac{1}{2}\sqrt{\frac{b_c^2}{2m_1^2} + \frac{k_c^2}{m_1^2}} \tag{35}$$

and the w_c corresponding value of time delay ,h_0 is:

$$h_0 = \frac{1}{\omega_c} tan^{-1}(\frac{b_c \omega_c}{k_c}) \tag{36}$$

Equation 34 can be used as a formula to select safe values, results in stable contact simulation, of contact parameters for a given time delay and reduced mass of satellites. For example, if HIL docking simulation control command has a time delay of h which indicates the closed-loop control will be unstable if the the value of h_0 is less than h.

5. RESULTS

SMART-OLEV [14] docking scenario is considered where the probe of the Chaser dock to the nozzle of the Target satellite. The simulator consists of satellites simulator, contact dynamics simulation and robot simulator. The satellites are simulated using the rigid body dynamics equations. The robot end-effector dynamics are modeled by the time delay of the robot controller.

5.1. 6-DOF Contact Simulation

Simulink simulation is developed to demonstrate that the docking simulator concept, based on hybrid contact model, can be used to perform contact tests in 6-DOF. In this simulation, both the measured part and the virtual part of the hybrid contact model are simulated. Fig 3 shows the frames used for the simulation. In order to perform active docking the Chaser satellite control bandwidth shall be more than the contact frequency. Thus, it will be necessary to have softer docking interface at the probe to decrease the bandwidth of contact. With this assumption, we choose softer desired contact parameters that has a normal stiffness equal to 3000N/m and zero damping to test the docking simulator.

Table 1. Initial parameters [$\boldsymbol{x}^{H,W}, \boldsymbol{v}_c^{D,T}, \boldsymbol{\omega}_c^{D,T}$ defined w.r.t frame G]

Parameters	Chaser	Target
$m[kg]$	750	1050
$I_{xx,yy,zz}[kg.m^2]$	$[812.5, 625,$ $312.5]$	$[1137.5, 875,$ $437.5]$
$\mathbf{x}^{H,W}[m]$	$[0.5, 0.78, 2.5]$	$[0.5, 0.6, 4.4]$
$\mathbf{r}_{DH,TW}[m]$	$[0, 0, 1.5]$	$[0, 0, 1.5]$
$\mathbf{v}_c^{D,T}[m/s]$	[0,0,0.05]	[0,0,0]
$\boldsymbol{\omega}_c^{D,T}[rad/s]$	[0,0,0]	[0,0,0]

In this example, we assumed that the probe attached at the Chaser is 1m long and 0.01m tip radius. In addition, the cone at Target satellite is 1m hight and 0.2m radius. The Target satellite contact profile is presented for net normal stiffness of $2000N/m$ for the virtual part and $1000N/m$ for the compliance device which gives a net stiffness of the desired 3000N/m. The damping is assumed zero. Table 1 presents the initial parameters used for this simulation where $I_{11,22,33}$ represents the principal moments of inertia of the satellites and $\mathbf{r}_{DH,TW}$ represents the vector from the **CoM** of the satellites to the docking interface (robot tool) frames.

Fig 7 shows the probe tip motion with respect to frame W where the the origin of frame *W* matched with the bottom of the cone. This figure also shows the contact status during the simulation period. The probe tip motion was only in the x-z plane because of the contact forces were detected in x-axis and z-axis only.

Fig 8 shows the contact forces and torques profile for the virtual and measured part of the Target satellite simulator. The implication of this simulation is that the user can tune the virtual contact parameters to perform different contact cases. Due to the misalignment between x-axis and y-axis, we detected contact forces in x-axis and z-axis and contact torque y-axis. A contact force in y-axis was not detected because there was no misalignment in y-axis between the probe tip and cone.

Fig 9 shows the sum of the virtual and measured contact forces and torques for each axis where each axis forces/torques are shown in Fig 8. The feedback input to the simulator was the sum of forces/torques from the virtual and measured contact forces/torques. This results the corresponding linear and angular velocities as shown in Fig 9.

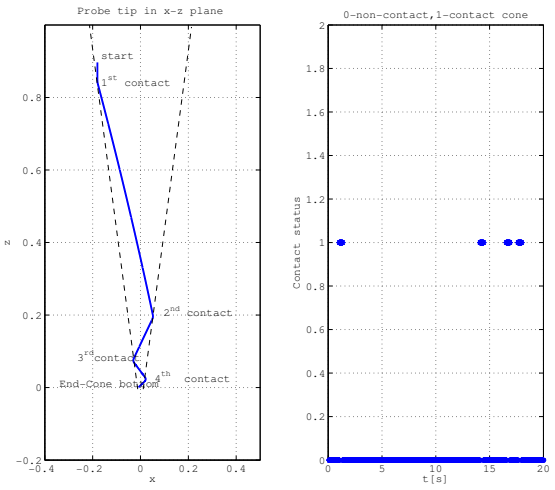

Figure 7. Probe tip motion w.r.t frame W(left) and contact status(right)

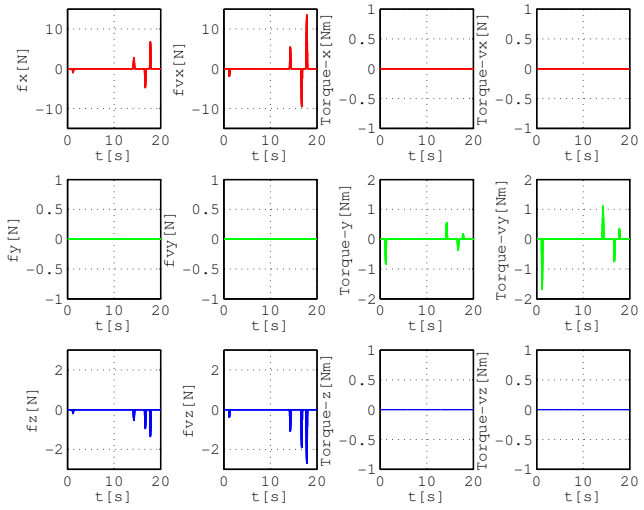

Figure 8. Target contact profile w.r.t frame W: $\boldsymbol{f}, \boldsymbol{\tau}$ is the measured part, $\boldsymbol{f}_v, \boldsymbol{\tau}_v$ is the virtual part

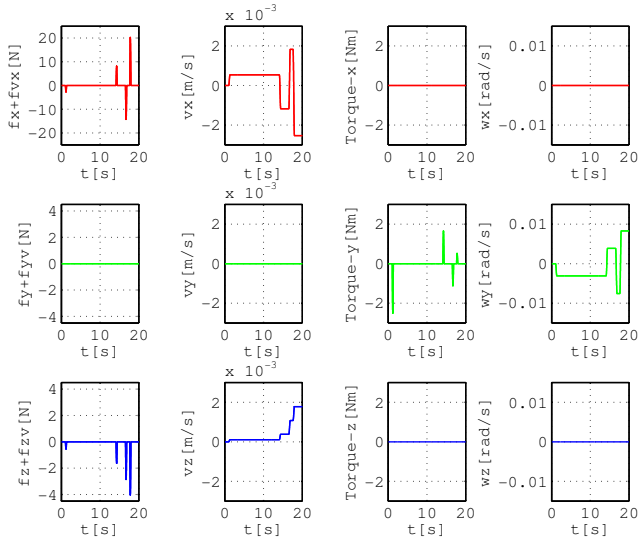

Figure 9. Target satellite simulator: total contact force $(\boldsymbol{f}_v^W + \boldsymbol{f}^W)$, $\boldsymbol{\nu}^G$, total torque$(\boldsymbol{\tau}^W + \boldsymbol{\tau}_v^W)$, and $\boldsymbol{\omega}^G$

5.2. Validating the stability region

In order to validate the stability region simulation is performed. The simulation were performed in 1-DOF by changing the contact parameters. The aim of this simulation was to validate the stability window of the simulator as a function of contact parameters, time delay and masses of the satellites.

When simulation was performed using the parameters $m_1 = 749.4kg$, $h = 16ms$, $k_c = 2500N/m$, $b_{cs} = 20Ns/m$ and $h_0 = 8ms$ which was computed using Eq. 36. The simulation was unstable as expected. However, when the damping was increased to 60Ns/m, the system became stable because of h_0 value increase from 8ms to 23.9ms and that is greater than h. Fig 10 shows the stability problem when there is no sufficient damping

to remove the added energy due to the time delay.

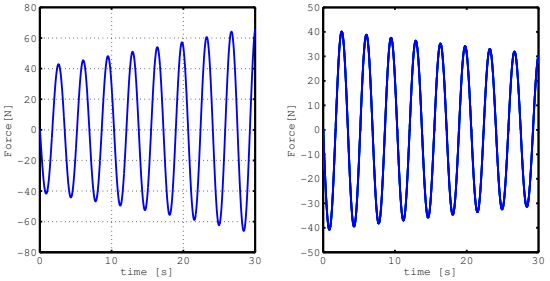

Figure 10. Left plot shows when b=20Ns/m (unstable) and right plot shows when b=60Ns/m (stable). Other parameters are kept constant.

6. CONCLUSION AND FUTURE WORK

With the presented tool for emulating contacts, it was demonstrated in simulation that HIL contact can be performed for a wide range of contact parameters, which does not include stiff contacts. Due to the introduction of a suitably tuned active impedance control element, in conjunction with a passive compliance, changes in the contact properties are achieved in software. This allows to test docking interfaces tools such as a probe by varying the virtual compliance where the real part is mounted between the Chaser satellite (robot end-effector) and the probe. Furthermore, it helps to develop a control algorithm for docking.

The passive compliance device has been designed as a component of the hybrid contact model. This device is designed to have minimum gravitational force impact on the force/torque sensor which allows to choose sensor that is more accurate.

We perform stability analysis of the closed-loop docking simulator to investigate the effect of time delay. The analysis indicates there is a limit to tune the contact parameters because of the time delay of robot controller. Thus, the docking simulator is stable for a range of contact parameters where the range varies depending on the mass of the satellites and the values of the desired contact parameters. A formula is derived that can be used to check wether the desired contact parameters are in the range of a stabile docking simulator for a known time delay of the controller.

In the future HIL docking simulator concept shall be demonstrated in the experiment for 6-DOF case.

ACKNOWLEDGMENTS

The authors acknowledges many fruitful discussions with Mr. Ranier Krenn of the DLR's Robotics and Mechatronics Institute.

REFERENCES

[1] J.L Schwartz, M.A. Peck, and C.D. Hall, "Historical review of air-bearing spacecraft simulation",AIAA Journal of GCD, Vol. 26,no. 4 pp 513-522,2003

[2] M. Zebenay, R. Lampariello, T. Boge, and D. Choukroun, A new contact dynamics model tool for Hardware-in-the-loop docking dimulation,i-SAIRAS2012 4-6 Sep 2012, Turin, Italy.

[3] T. Boge, T.Wimmer, O.Ma, M.Zebenay, EPOS-A Robotics-Based Hardware-in-the-Loop Simulator for Simulating Satellite RvD Operations, i-SAIRAS, Sapporo, Japan, August 29-September 1, 2010

[4] Rupp Th., Boge T., Kiehling R., Sellmaier F. "Flight Dynamics Challenges of the German On-Orbit Servicing Mission DEOS",21st International Symposium on Space Flight Dynamics, 28 Sep. - 2 Oct. 2009, Toulouse, France.

[5] F.D. Roe, R.T. Howard, and L. Murphy, Automated rendezvous and capture system development and simulation for NASA, Proc. SPIE, Vol. 5420, 118 (2004)

[6] O. Ma, J. Wang, S. Misra, and M. Liu, On the validation of SPDM task verification facility, Journal of Robotic Systems, Vol.21, No.5, 2004, pp. 219-235.

[7] Ou Ma, M. Zebenay, T. Boge, Control of an industrial robot for hardware-in-the-loop simulation of satellite docking . SPIE IV. 25 - 29 April 2011,Orlando, USA.

[8] K. Yoshida, H. Nakanishi, H.Ueno, N. Inaba, T. Nishimaki and M. Oda, "Dynamics, control and impedance matching for robotic capture of a non-cooperative satellite", advanced robotics 18,175198.

[9] Strzalko, J., Grabski, J., Perlikowski, P., Stefanski, A "Dynamics of Gambling: Origins of Randomness in Mechanical Systems", Springer, Page 23-29, 2009

[10] Kraus, P.R. and Kumar, V.,Compliant contact models for rigid body collisions, Robotics and Automation, 1997. Proceedings., 1997 IEEE,1382-1387 vol.2

[11] G.Gilardi, I.Sharf, Literature Survey of contact dynamics modeling, Mechanism and Machine Theory 37 Dept. of Mechanics Engineering, Victoria, Canada ,2002, 1213-1239.

[12] H. Nakanishi, Modeling and Control of Contact Dynamics for a Free-Flying Space Robot in Target Capture Operation,PhD report,Tohoku University, Japan,2010.

[13] J.E Marshall H. Goerecki A. Korytowski and K.Walton. "Time-Delay Systems Stability and Performance Criteria with Application", Ellis Horwood, London, 1 edition, 1992.

[14] Rainer Krenn, Gerd Hirzinger, "Contact Dynamics Simulation for Space Robotics Applications", IEEE/RSJ, 2008-22-09 2008-26-09, Nice, France.